

Figure S1

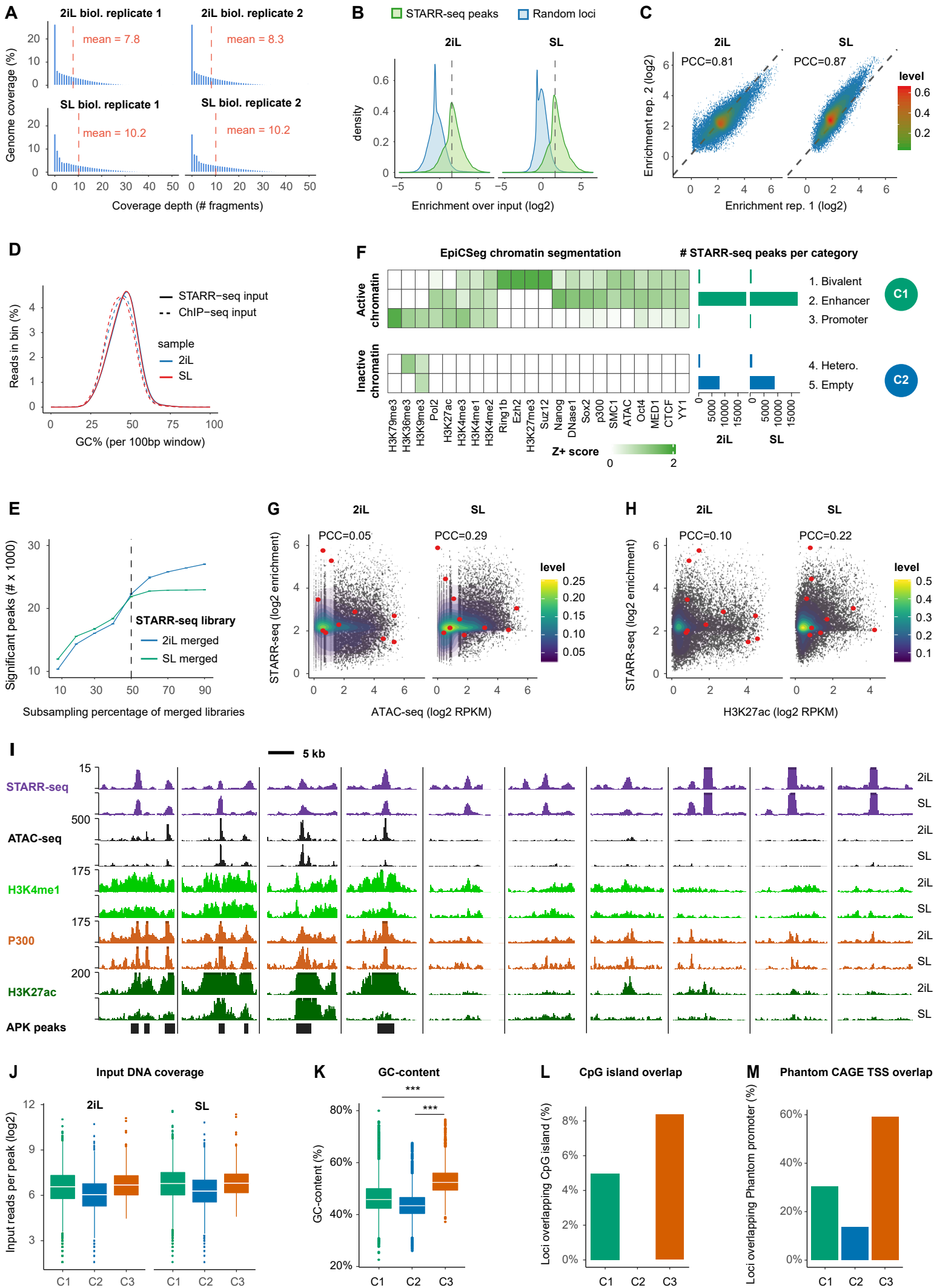


Figure S2

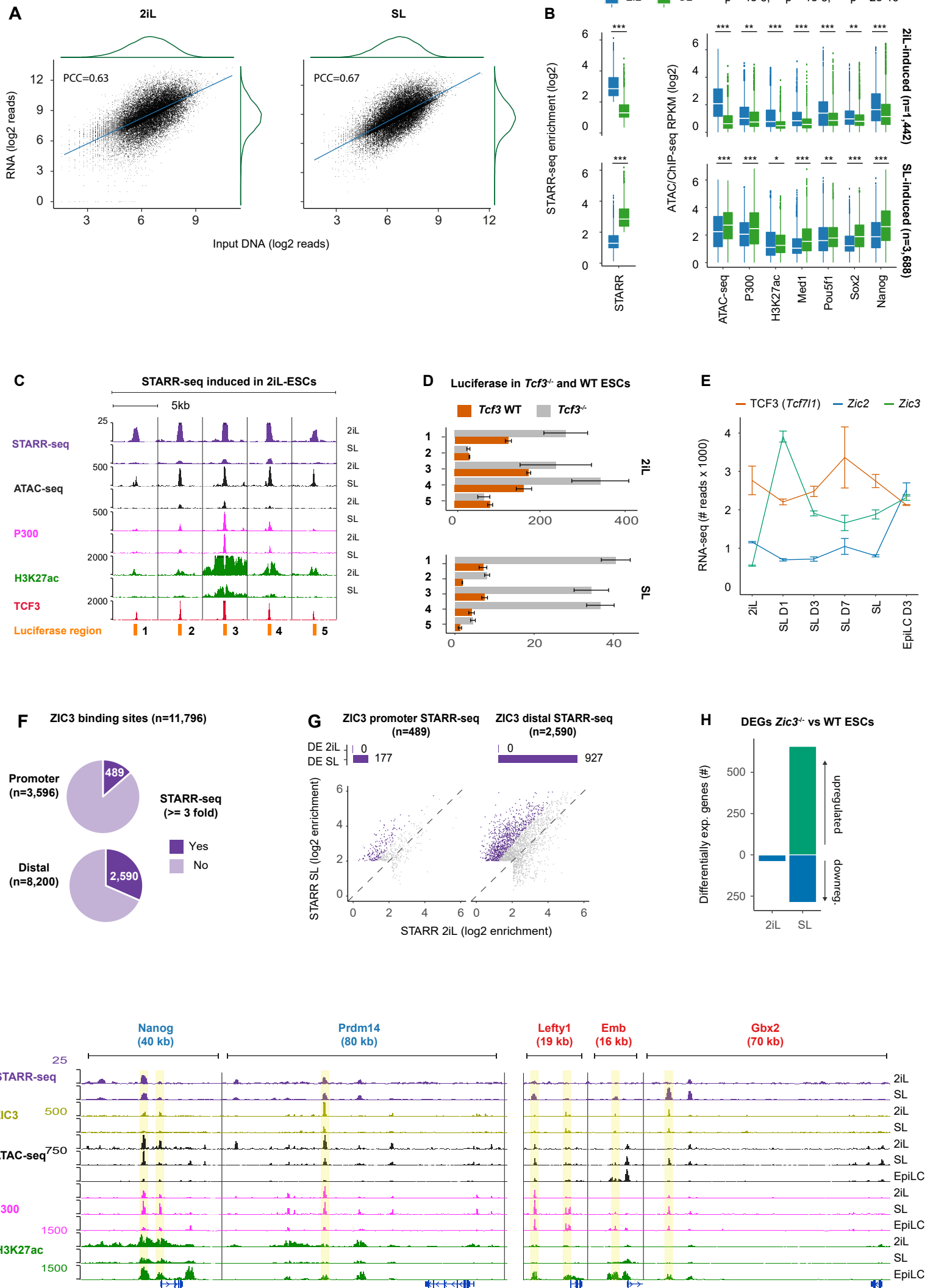


Figure S3

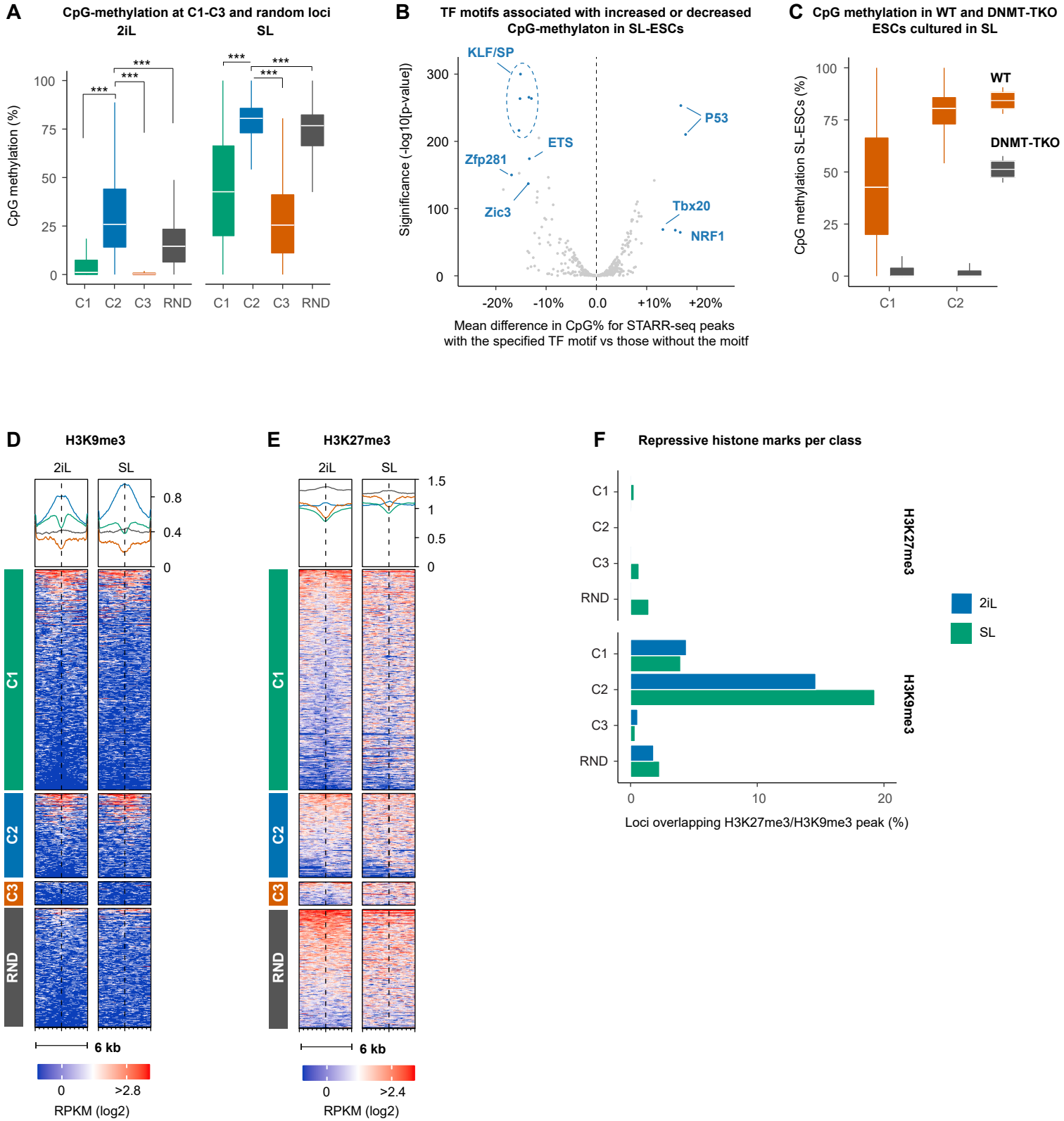
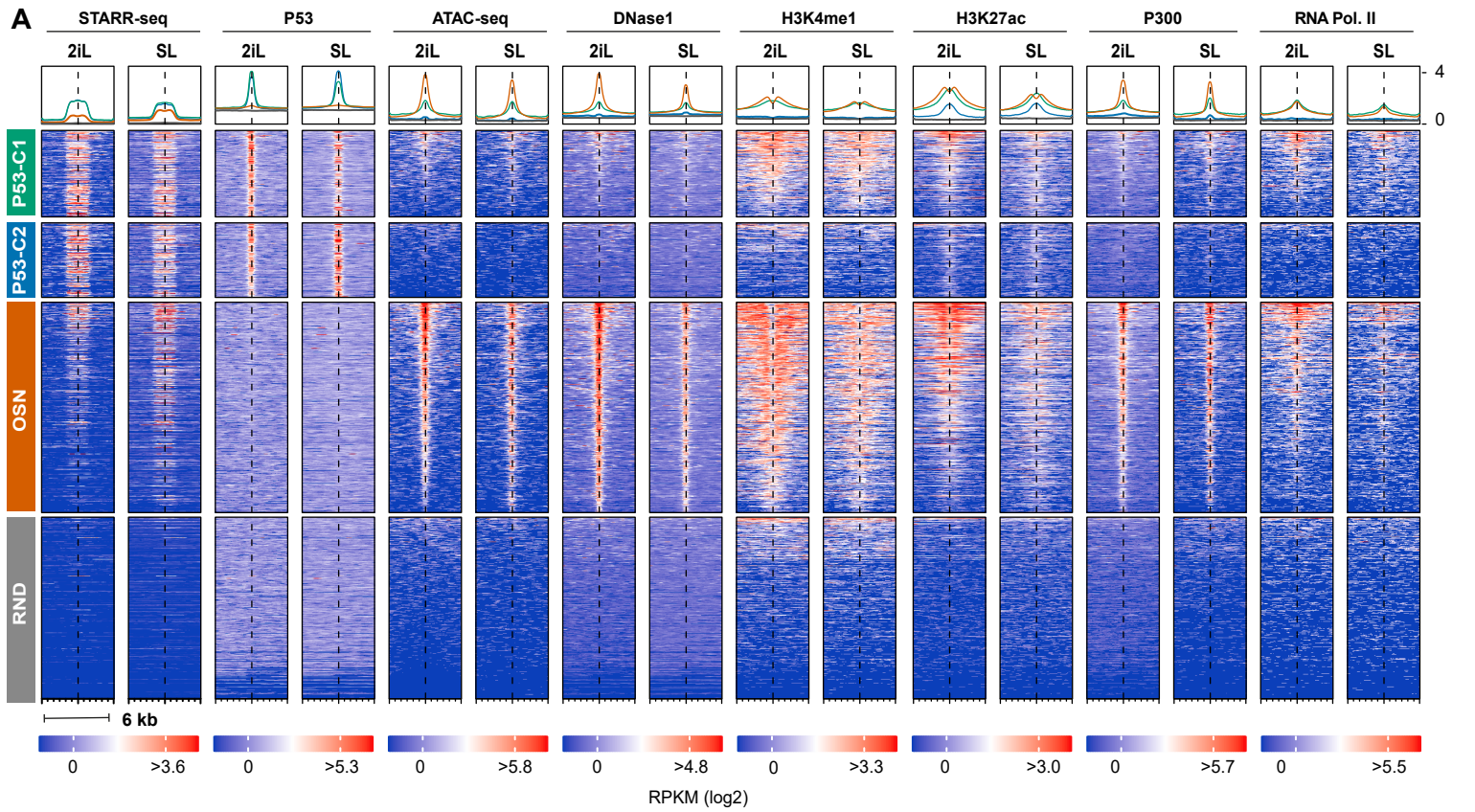
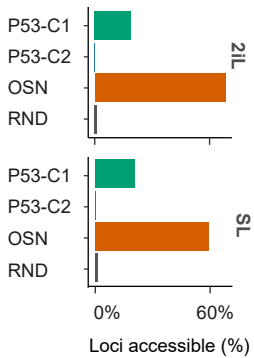


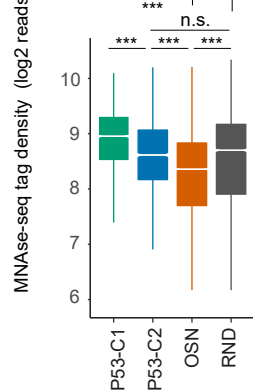
Figure S4



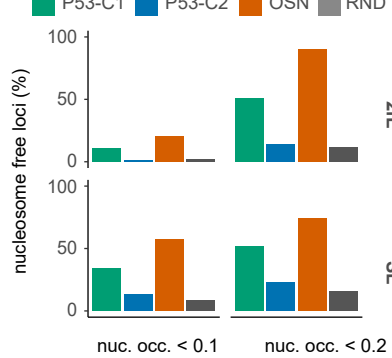
B ATAC-seq peaks



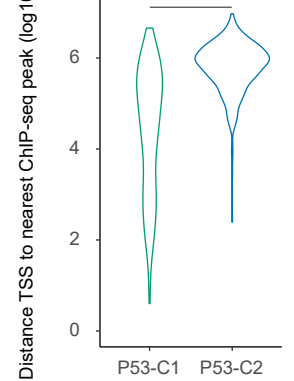
C MNase-seq tag density



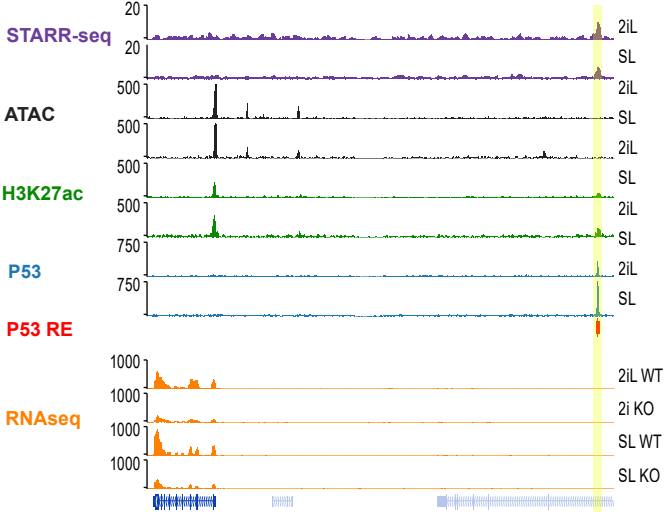
D Nucleosome free regions (NFR)



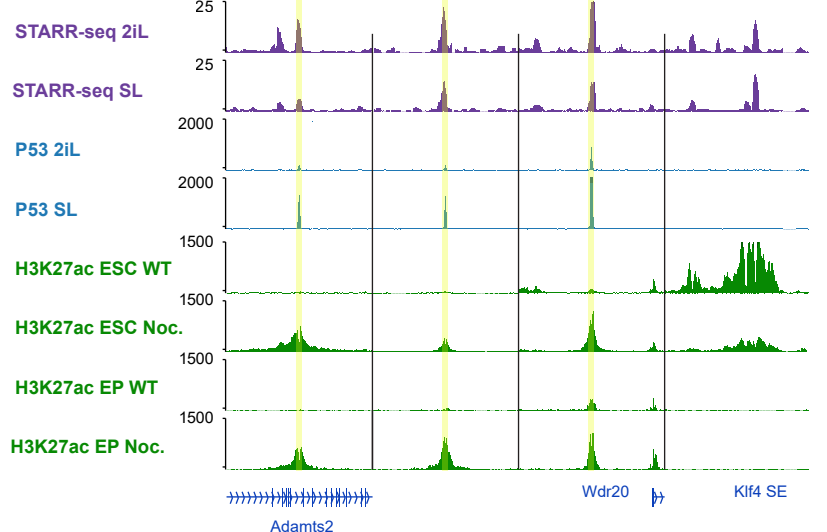
E Distance P53 target gene to nearest P53 peak



F Tmem184c (106 kb)



G



SUPPLEMENTARY FIGURE LEGENDS

Some of the panels in these supplemental figures contain public data. These panels are annotated with [PD]. The accession numbers of public data and their corresponding panels are annotated in Additional file 2: Table S1.

Figure S1: Quality assessment and chromatin-based classification of STARR-seq (lacking) loci.

- A.** Genome wide coverage and depth per STARR-seq input library.
- B.** STARR-seq enrichment at MACS2 peaks and randomly selected GC%-matched regions. A 3-fold or higher STARR-seq enrichment over input (dashed line) was observed in less than 3% of the randomly selected regions and used as a cutoff for significant enhancer signal.
- C.** Scatterplot of STARR-seq signal in biological replicate (rep.) 1 vs 2. PCC: Pearson's correlation coefficient.
- D.** Distribution of the GC% of DNA at STARR-seq peaks compared to ChIP-seq input libraries. GC% bias was computed from the mapped BAM files in 100bp windows across the mouse genome (see methods).
- E.** Number of STARR-seq peaks detected after merging the biological replicates and subsampling. The expected number of enhancers converges when ~60% of the reads in the merged libraries are sampled. Error bars denote the standard deviation of n=3 random subsamples.
- F.** **Left:** EpiCSeq chromatin segmentation of the mm9 genome into 5 clusters. Group 1-3 have active promoter/enhancer marks that are lacking at group 4-5. STARR-seq peaks overlapping a group 1-3 region are classified as C1 and largely overlap with the "enhancer" segments. STARR-seq regions that only overlap group 4-5 regions are classified as C2 and largely comprise "empty" segments enriched only for H3K9me3. For better visibility, columns were Z-scored and negative values were set to 0. **Right:** number of STARR-seq peaks assigned to each chromatin segment in 2iL or SL **[PD]**
- G.** Scatterplot of the ATAC-seq and STARR-seq enrichment at the C1-loci. ATAC-seq signal was computed at the STARR-seq summit flanked by 250bp on either side. PCC: Pearson's correlation coefficient. Ten red dots mark the values of the examples shown figure S1I.
- H.** Scatterplot of the H3K27ac and STARR-seq enrichment at C1-loci. H3K27ac signal was computed at the STARR-seq summit flanked by 2kb on both sides. PCC: Pearson's correlation coefficient. Ten red dots mark the values of the examples shown figure S1I.
- I.** Genome browser screenshots for C1 STARR-seq peaks with different levels of ATAC-seq, H3K27ac and STARR-seq enrichment. APK peak locations are indicated in the bottom (example 1-4). C1 STARR-seq peaks without a significant APK peak still show low

enrichment for H3K4me1, P300 or H3K27ac, but often lack a significant chromatin accessibility peak (example 5-10). Windows of 15kb are shown, centered on the STARR-seq peaks. See Additional file 3: Table S2 for genomic coordinates of these example loci.

- J. Boxplots of the number of input DNA fragments per class shows that the STARR-seq negative C3-loci have an equal or higher input count compared to the STARR-seq positive loci.
- K. Boxplot of the GC-content of C1-C3 loci (summit \pm 250 bp). *** $p < 2e-16$, Wilcoxon rank-sum test.
- L. Percentage of C1-C3 loci that overlap a CpG island annotated by the UCSC Table Browser (mm9). The overlap with the C2-class is below 1%.
- M. Percentage of C1-C3 loci that overlap a TSS annotated by the Phantom5 consortium.

Figure S2: TCF3 and ZIC3 are associated with STARR-seq peaks induced in 2iL- and SL-ESCs respectively.

- A. The strength of a STARR-seq peak correlates significantly with the coverage depth of the input library. This property is taken into consideration when calling differential STARR-seq peaks (see methods). Marginal densities are shown in green. PCC: Pearson's correlation coefficient.
- B. STARR-seq and ATAC-/ChIP-seq signal at 2iL- (n=1,442) and SL-induced (n=3,688) STARR-seq peaks of class C1. P-values: Wilcoxon's rank-sum test (two-sided) **[PD]**
- C. Examples of STARR-seq peaks with elevated signal in 2iL-ESCs. These loci are more accessible and have higher H3K27ac in 2iL-ESCs. TCF3 occupies these loci in SL-ESCs. The location of the luciferase primers (orange; see figure S2D and table S3) are shown in the bottom. **[PD]**
- D. Luciferase signal (Firefly/Renilla) scaled to F/R of a control region in WT and *Tcf3*^{-/-} ESCs for the five loci shown in figure S2C. Notice that the x-axis for SL is 10-fold lower compared to that of 2iL. See Table S3 for the genomic location and sequences of the primers that were used.
- E. RNA-seq expression of *Tcf3* (orange), *Zic2* (blue) and *Zic3* (green) during the transition from 2iL- to SL-ESCs and at SL cells that were converted to EpiLCs for 72h. Error bars denote the standard deviation of biological duplicates per time point.
- F. Union of ZIC3 binding sites in 2iL- and SL-ESCs (n=11,796). The number of peaks with significant STARR-seq enrichment ($FC \geq 3$ and $p < 0.05$; i.e. STARR-seq positive peaks) is annotated for promoter proximal and distal binding sites.
- G. Scatterplot of the STARR-seq signal at STARR-seq positive ZIC3 binding sites. The signal is highly skewed towards SL-ESCs and all differential STARR-seq peaks ($|FC| > 2.5$, $p < 0.05$; DESeq2) are found in that condition.

- H. Number of differentially expressed genes (DEGs, $|FC| \geq 2.5$ and $p < 0.05$) in *Zic3*^{-/-} vs WT ESCs.
- I. Browser screenshots of loci around genes annotated in figure 2L. The naïve pluripotency genes *Nanog* and *Prdm14* are expressed in 2iL- and SL-ESCs and have ZIC3-bound STARR-seq peaks (highlighted in yellow) in both conditions. *Lefty1*, *Emb* and *Gbx2* are cluster markers of SL-ESCs that lose expression upon genetic ablation of *Zic3*. These genes are associated with SL-specific STARR-seq peaks occupied by ZIC3. [PD]

Figure S3: C2-loci are active STARR-seq regions due to the absence of DNA methylation and repressive histone modifications.

- A. Boxplots of the average CpG methylation at C1-, C2-, C3-loci (summit ± 250 bp) and 50,000 CG%-matched random regions (RND) in 2iL- and SL-ESCs. *** $p < 2e-16$, Wilcoxon rank sum test. [PD]
- B. TF motifs whose presence (“yes” or “no”) is predictive of increased or decreased CpG-methylation at all STARR-seq peaks ($n=25,616$). CpG-methylation was measured in SL-cultured ESCs. STARR-seq peaks with a NRF1 or canonical P53 motif have on average 15-17% higher CpG-methylation in SL-ESCs compared to STARR-seq peaks lacking this P53 motif. Similarly, STARR-seq peaks with a ZIC3 motif have on average 14% less CpG-methylation in SL-ESCs than those lacking the ZIC3 motif. Average CpG-methylation was computed at the STARR-seq peak summit ± 250 bp. CpG-methylation changes were computed by single motif linear regression. P-values: t-test, corrected for testing $n=392$ motifs (Benjamini-Hochberg). [PD]
- C. CpG-methylation at C1 and C2 STARR-seq peaks in WT- and DNMT TKO ESCs cultured in SL. [PD]
- D. H3K9me3 at C1-C3 loci and 10,000 randomly selected regions. Read coverage was computed in tiles of 50bp in a region that flanks the STARR-seq summit (C1, C2) or ATAC-seq peak (C3) by 3kb on both sides. The average intensity (\log_2 RPKM) is shown in the top of the figure.
- E. H3K27me3 at C1-C3 loci and 10,000 randomly selected regions. Read coverage was computed in tiles of 50bp in a region that flanks the STARR-seq summit (C1, C2) or ATAC-seq peak (C3) by 3kb on both sides. The average intensity (\log_2 RPKM) is shown in the top of the figure.
- F. Percentage of C1, C2, C3 or randomly sampled regions that intersect a H3K27me3 (top) or H3K9me3 (bottom) peak in 2iL or SL. For C1-, C2- and C3-loci we used the peak summit flanked by 250bp on both sides. 10,000 GC%- and size matched regions were sampled from the mouse genome.

Figure S4: P53-bound STARR-seq loci are characterized by low chromatin accessibility and are categorized into active (class C1) and inactive enhancers (class C2) based on the presence/absence of active histone modifications.

- A.** STARR-seq, P53 occupancy and a number of enhancer marks at P53-C1, P53-C2, OSN-bound and randomly selected loci. Notice that P53-C2 loci lack all enhancer marks except STARR-seq, whereas P53-C1 regions have H3K4me1, H3K27ac and Pol II, but are also minimally accessible. The heatmap was sorted by descending ATAC-seq signal (2iL). The color gradient depicts the RPKM (log₂) of reads in tiles of 50bp. **[PD]**
- B.** Percentage of P53-C1, P53-C2, OSN-bound or randomly selected loci that intersect an ATAC-seq peaks (IDR < 0.03). **[PD]**
- C.** MNase-seq nucleosome summit values (computed with Danpos2) for the nucleosome closest to a P53-C1, P53-C2, OSN- or randomly selected peak. For P53-C1 and P53-C2 the nucleosome with highest MNase-seq signal within 74bp from the canonical P53 motif were considered. For OSN- and randomly selected regions, the highest signal within 74bp from the peak center was used. *** p < 2e-16, n.s.: not significant; Wilcoxon rank-sum test. **[PD]**
- D.** Percentage of P53-C1, P53-C2, OSN- and randomly selected loci for which the peak summit overlaps a nucleosome free region (NFR) in 2iL- or SL. NFRs were computed using NucleoATAC with the default settings (occ=0.1) and a relaxed (occ=0.2) nucleosome occupancy (nuc. occ.) cutoff (see methods).
- E.** Distance distribution of P53 target genes (FC < -2.5 and p < 0.05 in *Trp53*^{-/-} vs WT; DESeq2) to the nearest P53-C1 or P53-C2 ChIP-seq peak. *** p < 2e-16, Wilcoxon rank-sum test.
- F.** *Tmem184c* loses expression in *Trp53*^{-/-} compared to WT ESCs. The distal P53 binding site (yellow highlight) has minimal ATAC-seq accessibility compared to the *Tmem184* promoter region, but is (lowly) enriched for H3K27ac **[PD]**
- G.** P53-C2 STARR-seq peaks that gain H3K27ac after treatment with Nocodazole (Noc.) in ESCs and erythrocyte progenitors (EP). The OSN-bound superenhancer near *Klf4* (OSN control) is an active C1-enhancer that is not bound by P53. This enhancer loses, rather than gains H3K27ac after treatment with Nocodazole.